# Optothermal Properties of Fibers. XIV. Investigation of Some Optical Structural Parameters of Annealed and Cold Drawn Polyester Fibers

**I. M. FOUDA, M. A. KABEEL, F. M. EL-SHARKAWY**

Physics Department of Science, Mansoura University, Mansoura, Egypt

*Received 16 July 1997; accepted 26 October 1997*

**ABSTRACT:** Two-beam interferometry and density methods previously measured are used to study the changes in optical properties of annealed and cold drawn polyester (PET) fibers. Some structural parameters in the present work are determined, such as form birefringence, the number of molecules per unit volume, the virtual refractive index, the harmonic mean polarizability of the dielectric, the harmonic mean specific refractivity, and the isotropic refractive index. Also, the distribution of segment at an angle with respect to the draw ratio and the electric polarizability constant ($\Delta\alpha/3\alpha_0$) are determined. The generalized Lorentz–Lorenz equation given by de Vries is used to determine PET fiber structure parameters. Comparison between the results have been made with the Hermans optical orientation function. © 1998 John Wiley & Sons, Inc. J Appl Polym Sci 69: 33–44, 1998

**Key words:** polyester; density; draw ratio; orientation; crystallinity and annealed

## INTRODUCTION

Optical measurements play an important role in the characterization of synthetic and natural fibers. The importance of studying various optical properties, such as refractive indices and birefringence, for fibers leads to much accurate information to correlate the structural orientation properties of these fibers with their physical, chemical, mechanical, and thermal properties.[1–8]

Poly(ethylene terephthalate) (PET) is one of the most important commercially produced polyesters. As a uniaxially oriented fiber, it is used in textiles, and, as a biaxially oriented film, it is used as the substrate for magnetic recording media and photographic film, as a capacitor dielectric, and in shrinkable packaging material.[9] The morphology of unoriented PET, uniaxially oriented fiber, and biaxially oriented film has been studied extensively. The maximum degree of crystallinity normally attained is between 50 and 60%. The state of the noncrystalline material has been shown to depend strongly on the temperature of crystallization and the thermal treatment.[9]

Recently, application of two or multiple-beam interference to determine the optical parameters of synthetic and natural fibers are used.[10–14] Characterization of these fibers is important for the textile industry and the end use.

In this work, the optical and density results for samples of PET having different annealing conditions (previously measured interferometrically using two-beam and acoustic techniques[15–16]) are utilized to calculate some structural parameters. Relationships are given between optical and structural parameters.

## THEORETICAL CONSIDERATIONS

The mean values of the refractive indices of the fiber and the total mean birefringence were calcu-

*Correspondence to:* I. M. Fouda.

Journal of Applied Polymer Science, Vol. 69, 33–44 (1998)
 CCC 0021-8995/98/010033-12

lated from the totally duplicated and nonduplicated images of the fiber using Pluta interference microscope.[17–19]

The experimental values of the mean polarizabilities per unit volume parallel $\bar{P}_a^{\parallel}$ and perpendicular $\bar{P}_a^{\perp}$ to the fiber axis were derived from the measured values of the refractive index by application of the following Lorentz–Lorenz equations:

$$\bar{P}_{\parallel} = \frac{3}{4\pi}\left(\frac{n_{\parallel}^2 - 1}{n_{\parallel}^2 + 2}\right) \tag{1a}$$

$$\bar{P}_{\perp} = \frac{3}{4\pi}\left(\frac{n_{\perp}^2 - 1}{n_{\perp}^2 + 2}\right) \tag{1b}$$

These values are used in the following equation[20] to calculate the number of molecules per unit volume:

$$\Delta n = \frac{2\pi N}{\bar{n}}\left(\frac{\bar{n}^2 + 2}{3}\right)^2 (\bar{P}_{\parallel} - \bar{P}_{\perp}) \tag{2}$$

where $N$ is the number of molecules per unit volume, and $\bar{n}$ is the mean refractive index of the sample, which considered $\bar{n} = \left(\frac{n_{\parallel} + n_{\perp}}{2}\right)$, and $(\bar{P}_{\parallel} - \bar{P}_{\perp})$ equals the mean polarizabilities of the macromolecules for the same direction of the mean refractive indices.

Also, the calculation of the form birefringence could be obtained by the following equation,[21] in which the total birefringence is the sum of three contributions

$$\Delta n = \chi_c \Delta n_c + (1 - \chi_c)\Delta n_a + \Delta n_f \tag{3}$$

where $\Delta n$ is the total birefringence, $\Delta n_c$ is the birefringence of crystalline material and equals 0.22,[22] $\Delta n_a$ is the birefringence of amorphous material and equals 0.27,[22] $\Delta n_f$ is the birefringence of form material, and $\chi$ the volume fraction of crystalline regions.

## MEAN POLARIZABILITY OF THE MONOMER UNIT

The polarizability of a monomer unit like the polarizability of a simple organic molecule usually differs in different directions. As the refractive index of a polymer depends on the total polarizability of the molecules, this leads to the Lorentz–Lorenz by the following equation:

$$\frac{n_{\parallel}^2 - 1}{n_{\parallel}^2 + 2} = \frac{N_{(1)}\alpha^{\parallel}}{3\psi} \tag{4}$$

An analogous formula can be used for $n_a^{\perp}$, where $n_a^{\parallel}$ and $n_a^{\perp}$ are the mean refractive indices of the fiber for light vibrating parallel and perpendicular to the fiber axis, respectively.

$$\frac{\bar{n}^2 - 1}{\bar{n}^2 + 2} = \frac{N_{(1)}\bar{\alpha}}{3\psi} \tag{5}$$

where $\psi$ is the permitivity of free space = $8.85 \times 10^{-12}$ $\mathrm{Fm}^{-1}$, and $\bar{\alpha}$ is the mean polarizability of a monomer unit.

For a bulk polymer of density $\rho$ and monomer unit molecular weight $M$, the number of monomer units per unit volume, which also equal the number of carries of the dipole moment, $N_{(1)} = \frac{N_A \rho}{M}$ where $N_A$ is Avogadro's number, $6.02 \times 10^{23}$, and $M$ for PET = 192.[23]

De Vries[24] gave a theory on the basis of an internal field with the aid of classical electromagnetic theory, in which he generalized the Lorentz–Lorenz equation; so for monochromatic light, the well-known Lorentz–Lorenz equation becomes

$$\frac{n^2 - 1}{n^2 + 2} = \frac{N_{(1)}\alpha}{3\psi} \tag{6}$$

The right-hand side of eq. (6) is proportional to the density $\rho$ ($\mathrm{Kg/m}^3$) of the medium and may also be written as

$$\frac{n^2 - 1}{n^2 + 2} = \varepsilon\rho \tag{7}$$

where $\epsilon$ ($\mathrm{m}^3/\mathrm{Kg}$) is called the specific refractivity of the isotropic dielectric. Writing this equation for fibers in its parallel and transverse components, the generalized Lorentz–Lorenz equations are as follows:

$$\frac{n_{\parallel}^2 - 1}{n_{\parallel}^2 + 2} = \frac{N_{(1)}\alpha^{\parallel}}{3\psi} = \varepsilon_{\parallel}\rho \tag{8}$$

An analogous formula can also be derived for $n_a^{\perp}$.

Also, de Vries defined the invariant refractive index, which he call the "virtual refractive index" $n_v$ by

**Table I(a) Refractive Indices $n_a^{\parallel}$ and $n_a^{\perp}$, Total Birefringence $\Delta n_a$, Polarizabilities $P^{\parallel}$, $P^{\perp}$ and $\Delta P$, The Number of Molecules Per Unit Volume $N$, and the Number of Random Links Per Chain $N_{(2)}$ at A Constant Annealing Temperature (120 ± 1°C)**

| Draw Ratio | $n_a^{\parallel}$ | $n_a^{\perp}$ | $\Delta n_a$ | $P^{\parallel}$ | $P^{\perp}$ | $\Delta P$ | $N$ | $N_{(2)}$ |
|---|---|---|---|---|---|---|---|---|
| 1.00 | 1.673 | 1.573 | 0.1000 | 0.0894 | 0.0786 | 0.0108 | 23.5 | 3.2 |
| 1.16 | 1.674 | 1.568 | 0.1066 | 0.0896 | 0.0781 | 0.0115 | 23.5 | 3.2 |
| 1.32 | 1.683 | 1.558 | 0.1242 | 0.0905 | 0.0770 | 0.0135 | 23.5 | 3.2 |
| 1.48 | 1.693 | 1.556 | 0.1371 | 0.0915 | 0.0767 | 0.0148 | 23.5 | 3.2 |
| 1.64 | 1.696 | 1.551 | 0.1442 | 0.0918 | 0.0762 | 0.0156 | 23.5 | 3.2 |
| 1.80 | 1.700 | 1.550 | 0.1499 | 0.0923 | 0.0761 | 0.0162 | 23.5 | 3.2 |
| 1.96 | 1.704 | 1.548 | 0.1562 | 0.0927 | 0.0758 | 0.0169 | 23.5 | 3.2 |
| 2.12 | 1.706 | 1.541 | 0.1647 | 0.0929 | 0.0751 | 0.0178 | 23.5 | 3.2 |
| 2.28 | 1.710 | 1.539 | 0.1715 | 0.0933 | 0.0748 | 0.0185 | 23.5 | 3.2 |

**Table I(b) Refractive Indices $n_a^{\parallel}$ and $n_a^{\perp}$, Total Birefringence $\Delta n_a$, Polarizabilities $P^{\parallel}$, $P^{\perp}$ and $\Delta P$, The Number of Molecules Per Unit Volume $N$, and the Number of Random Links Per Chain $N_{(2)}$ at A Constant Annealing Temperature (140 ± 1°C)**

| Draw Ratio | $n_a^{\parallel}$ | $n_a^{\perp}$ | $\Delta n_a$ | $P^{\parallel}$ | $P^{\perp}$ | $\Delta P$ | $N$ | $N_{(2)}$ |
|---|---|---|---|---|---|---|---|---|
| 1.00 | 1.676 | 1.568 | 0.1074 | 0.0898 | 0.0781 | 0.0117 | 23.5 | 5.6 |
| 1.16 | 1.676 | 1.560 | 0.1160 | 0.0898 | 0.0772 | 0.0126 | 23.5 | 5.6 |
| 1.32 | 1.684 | 1.560 | 0.1240 | 0.0906 | 0.0772 | 0.0134 | 23.5 | 5.6 |
| 1.48 | 1.686 | 1.560 | 0.1259 | 0.0908 | 0.0772 | 0.0137 | 23.5 | 5.6 |
| 1.64 | 1.688 | 1.554 | 0.1346 | 0.0911 | 0.0765 | 0.0146 | 23.5 | 5.6 |
| 1.80 | 1.696 | 1.553 | 0.1431 | 0.0919 | 0.0764 | 0.0155 | 23.5 | 5.6 |
| 1.96 | 1.699 | 1.553 | 0.1461 | 0.0922 | 0.0764 | 0.0158 | 23.5 | 5.6 |
| 2.12 | 1.700 | 1.553 | 0.1470 | 0.0946 | 0.0763 | 0.0184 | 23.5 | 5.6 |
| 2.28 | 1.702 | 1.552 | 0.1499 | 0.0924 | 0.0763 | 0.0162 | 23.5 | 5.6 |
| 2.44 | 1.703 | 1.550 | 0.1535 | 0.0926 | 0.0760 | 0.0166 | 23.5 | 5.6 |

**Table I(c) Refractive Indices $n_a^{\parallel}$ and $n_a^{\perp}$, Total Birefringence $\Delta n_a$, Polarizabilities $P^{\parallel}$, $P^{\perp}$ and $\Delta P$, The Number of Molecules Per Unit Volume $N$, and the Number of Random Links Per Chain $N_{(2)}$ at A Constant Annealing Temperature (160 ± 1°C)**

| Draw Ratio | $n_a^{\parallel}$ | $n_a^{\perp}$ | $\Delta n_a$ | $P^{\parallel}$ | $P^{\perp}$ | $\Delta P$ | $N$ | $N_{(2)}$ |
|---|---|---|---|---|---|---|---|---|
| 1. | 1.673 | 1.560 | 0.1164 | 0.0898 | 0.0772 | 0.0126 | 23.5 | 2.7 |
| 1.16 | 1.687 | 1.555 | 0.1316 | 0.0909 | 0.0766 | 0.0143 | 23.5 | 2.7 |
| 1.32 | 1.691 | 1.552 | 0.1388 | 0.0913 | 0.0763 | 0.0150 | 23.5 | 2.7 |
| 1.48 | 1.700 | 1.549 | 0.1497 | 0.0922 | 0.0760 | 0.0162 | 23.5 | 2.7 |
| 1.64 | 1.703 | 1.544 | 0.1582 | 0.0925 | 0.0754 | 0.0171 | 23.5 | 2.7 |
| 1.8 | 1.709 | 1.542 | 0.1672 | 0.0932 | 0.0751 | 0.0181 | 23.5 | 2.7 |
| 1.96 | 1.713 | 57.93 | 0.1749 | 0.0936 | 0.0747 | 0.0189 | 23.5 | 2.7 |

$$n_v = \sqrt{1 + \frac{3[n_{\parallel}^2 - 1][n_{\perp}^2 - 1]}{[n_{\perp}^2 - 1] + 2[n_{\parallel}^2 - 1]}} \qquad (9)$$

where the virtual refractive index $n_v$ replaces the isotropic refractive index equation,

$$n_{\mathrm{iso}_{(1)}} = \frac{(n_a^{\parallel} + 2n_a^{\perp})}{3} \qquad (10)$$

and these equations [eq. (9)] lead to the harmonic mean polarizability of the dielectric $\alpha_v$ by the following equation:

$$\alpha_v = \frac{3\psi}{N_{(1)}} \cdot \frac{n_v^2 - 1}{n_v^2 + 2} \qquad (11)$$

Likewise, for the harmonic mean specific refractivity, we have

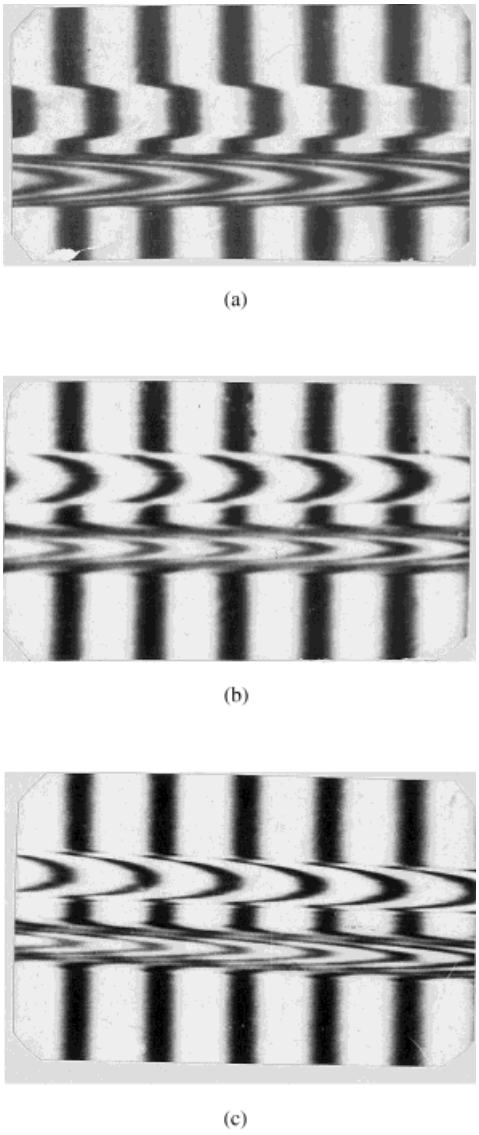

**Plate 1** (a)–(c) Microinterfrograms of a totally duplicated image of PET fiber at different draw ratios with annealing temperatures of 120, 140, and 160°C ($\lambda$ = 546 nm) in a parallel direction.

$$\varepsilon_v = \rho^{-1} \cdot \frac{n_v^2 - 1}{n_v^2 + 2} \tag{12}$$

In a recent approach to the continuum theory of birefringence of oriented polymer,[24] it was found that the value of $F_\theta$ is as follows:

$$F_\theta = \left[\frac{n_1^2 n_2^2}{n_\parallel^2 n_\perp^2}\right] \cdot \left[\frac{n_\parallel + n_\perp}{n_1 + n_2}\right] \cdot \frac{\Delta n_a}{\Delta n_{\max}} \tag{13}$$

which is slightly different from the original simple expression for the degree of orientation used by Hermans,[25] as follows:

$$F_\Delta = \frac{\Delta n}{\Delta n_{\max}}$$

Hermans optical orientation function $F_\Delta$ ($F_\Delta = \langle P_2(\theta)\rangle$) has been corrected by de Vries to be $F_\theta$ in the range $0 < \Delta n < 0.8$ as

$$F_\theta = (1 + a)F_\Delta - aF_\Delta^2$$

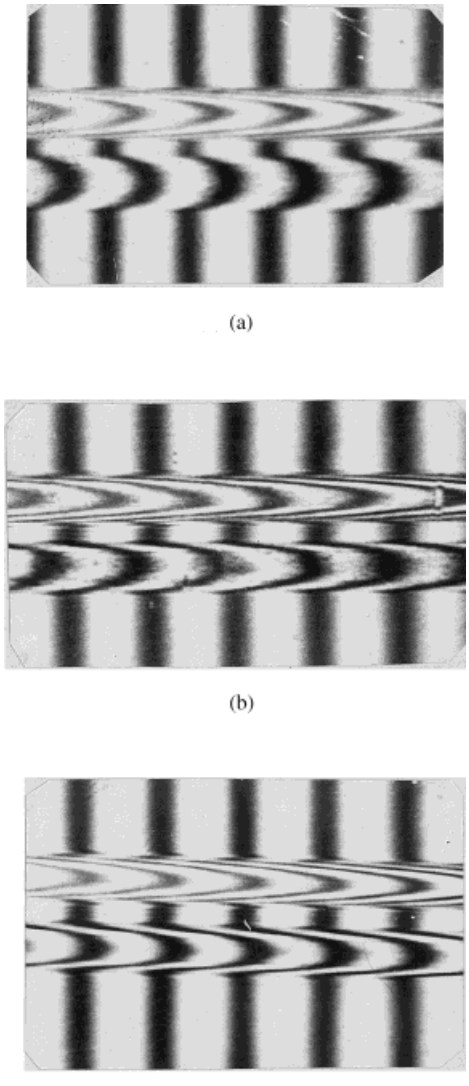

**Plate 2** (a)–(c) Microinterfrograms of a totally duplicated image of PET fiber at different draw ratios with annealing temperatures of 120, 140, and 160°C ($\lambda$ = 546 nm) in a perpendicular direction.

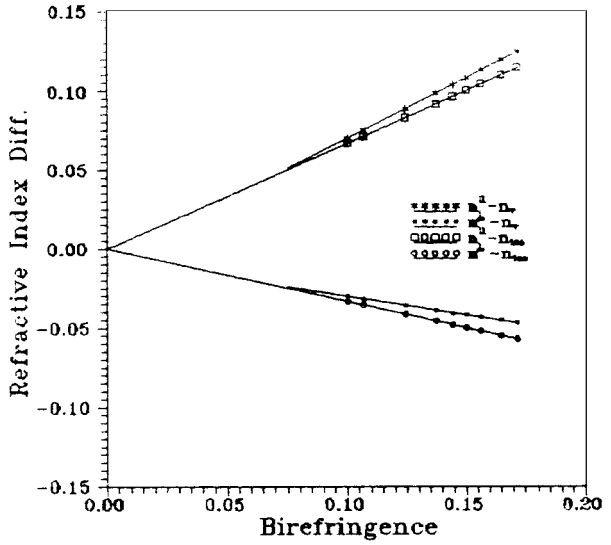


(a)

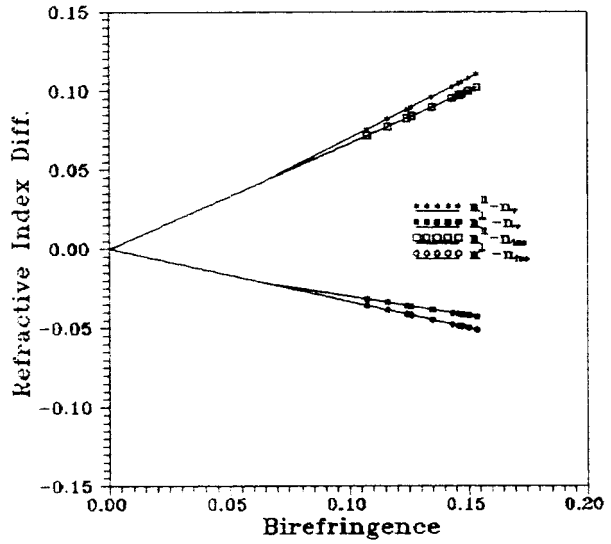


(b)

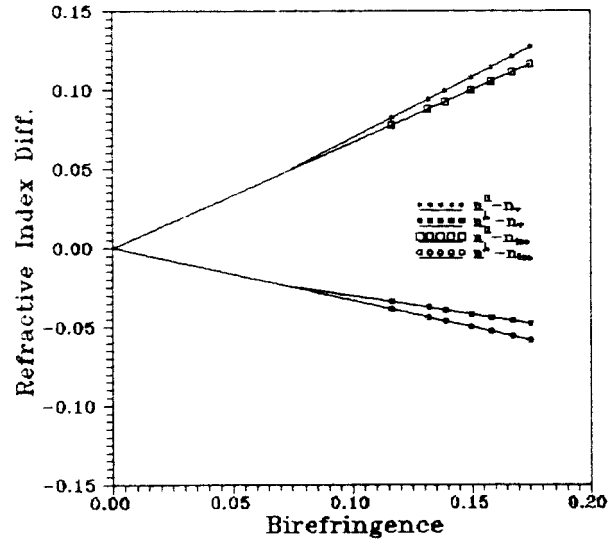


(c)

where

$$(1 + a) = \frac{2n_1^2 n_2^2}{n_v^2(n_1 + n_2)} \tag{14}$$

where $n_1$, $n_2$, and $n_v$ are given from de Vries[24] and $n_v \cong n_{\text{iso}}$ and are evaluated from eq. (10). So the constant $a$ was calculated and found to be 0.9. Also, the specific refractivity $\epsilon_i$ in a certain direction $i$, can be determined by the following equations[24] considering the anisotropy index:

$$\frac{n_\parallel^2 - 1}{n_\parallel^2 + 2 + S(n_\parallel^2 - 1)} = \varepsilon_\parallel \rho \tag{15a}$$

and

$$\frac{n_\perp^2 - 1}{n_\perp^2 + 2 + S(n_\perp^2 - 1)} = \varepsilon_\perp \rho \tag{15b}$$

where $\rho$ is the density and $S$ the anisotropy index and equal for PET $= -0.57$.[24]

The optical orientation function and orientation angle can be calculated using the Hermans equation,[25] as follows:

$$F_\theta = \frac{\Delta n_a}{\Delta n_{\max}} \tag{16}$$

The value of $\Delta n_{\max}$ has been previously determined to be[24] 0.24 for perfectly (or fully) oriented fiber, and $\Delta n_a$ is the measured mean birefringence.

In evaluating the orientation function for partially oriented aggregate, $\langle P_2(\theta)\rangle$ is defined by Ward[26] by the following equation:

$$\langle P_2(\theta)\rangle = \frac{\Delta n_a}{\Delta n_{\max}} \tag{17}$$

which is the same function named by Hermans.[25]

Cunningham et al.[27] derived a relation between the optical orientation function $\langle P_2(\theta)\rangle$ and the polarizability, as follows:

$$\frac{\Phi^\parallel - \Phi^\perp}{\Phi^\parallel + 2\Phi^\perp} = \left(\frac{\Delta\alpha}{3\alpha_0}\right)\langle P_2(\theta)\rangle \tag{18}$$

**Figure 1** (a)–(c) Relations between the birefringence $\Delta n$ and the refractive index differences ($n^\parallel - n_v$, $n^\perp - n_v$, $n^\parallel - n_{\text{iso}}$, and $n^\perp - n_{\text{iso}}$) of fiber at different draw ratios at 120, 140, and 160°C.

**Table II(a) Density $\rho$, Crystallinity $\chi$, $(1 - \chi)$, Form Birefringence $\Delta n_f$, Isotropic Refractive Indices, and Virtual Refractive Index $n_v$ at A Constant Annealing Temperature (120 ± 1°C)**

| Draw Ratio | $\rho$ | $\chi$ (%) | $(1 - \chi)$ (%) | $\Delta n_f$ | $n_{iso(1)}$ | $n_{iso(2)}$ | $n_v$ |
|---|---|---|---|---|---|---|---|
| 1.00 | 1.395 | 49.09 | 50.91 | −0.145 | 1.6058 | 1.5735 | 1.6022 |
| 1.16 | 1.391 | 45.21 | 54.79 | −0.141 | 1.6033 | 1.5734 | 1.5992 |
| 1.32 | 1.384 | 39.75 | 60.25 | −0.126 | 1.5998 | 1.5731 | 1.5942 |
| 1.48 | 1.387 | 42.07 | 57.93 | −0.112 | 1.6013 | 1.5728 | 1.5946 |
| 1.64 | 1.383 | 39.09 | 60.91 | −0.106 | 1.5994 | 1.5726 | 1.5919 |
| 1.80 | 1.385 | 40.50 | 59.50 | −0.100 | 1.6003 | 1.5725 | 1.5923 |
| 1.96 | 1.384 | 39.59 | 60.41 | −0.094 | 1.6000 | 1.5723 | 1.5910 |
| 2.12 | 1.378 | 34.38 | 65.62 | −0.088 | 1.5963 | 1.5721 | 1.5867 |
| 2.28 | 1.377 | 33.88 | 66.12 | −0.082 | 1.5960 | 1.5719 | 1.5856 |

**Table II(b) Density $\rho$, Crystallinity $\chi$, $(1 - \chi)$, Form Birefringence $\Delta n_f$, Isotropic Refractive Indices, and Virtual Refractive Index $n_v$ at A Constant Annealing Temperature (140 ± 1°C)**

| Draw Ratio | $\rho$ | $\chi$ (%) | $(1 - \chi)$ (%) | $\Delta n_f$ | $n_{iso(1)}$ | $n_{iso(2)}$ | $n_v$ |
|---|---|---|---|---|---|---|---|
| 1 | 1.392 | 46.53 | 53.47 | −0.139 | 1.6042 | 1.5734 | 1.6000 |
| 1.16 | 1.382 | 38.35 | 61.65 | −0.135 | 1.5987 | 1.5730 | 1.5938 |
| 1.32 | 1.387 | 42.15 | 57.85 | −0.125 | 1.6013 | 1.5731 | 1.5958 |
| 1.48 | 1.388 | 43.14 | 56.86 | −0.123 | 1.6020 | 1.5730 | 1.5963 |
| 1.64 | 1.382 | 37.69 | 62.31 | −0.117 | 1.5985 | 1.5728 | 1.5919 |
| 1.8 | 1.386 | 41.49 | 58.51 | −0.106 | 1.6009 | 1.5726 | 1.5936 |
| 1.96 | 1.387 | 42.23 | 57.77 | −0.103 | 1.6014 | 1.5726 | 1.5938 |
| 2.12 | 1.387 | 42.40 | 57.60 | −0.102 | 1.6015 | 1.5726 | 1.5938 |
| 2.28 | 1.388 | 42.81 | 57.19 | −0.099 | 1.6018 | 1.5725 | 1.5938 |
| 2.44 | 1.386 | 41.24 | 58.76 | −0.096 | 1.6008 | 1.5724 | 1.5924 |

**Table II(c) Density $\rho$, Crystallinity $\chi$, $(1 - \chi)$, Form Birefringence $\Delta n_f$, Isotropic Refractive Indices, and Virtual Refractive Index $n_v$ at A Constant Annealing Temperature (160 ± 1°C)**

| Draw Ratio | $\rho$ | $\chi$ (%) | $(1 - \chi)$ (%) | $\Delta n_f$ | $n_{iso(1)}$ | $n_{iso(2)}$ | $n_v$ |
|---|---|---|---|---|---|---|---|
| 1.00 | 1.382 | 37.93 | 62.07 | −0.135 | 1.5986 | 1.5732 | 1.5937 |
| 1.16 | 1.382 | 38.18 | 61.82 | −0.119 | 1.5988 | 1.5729 | 1.5925 |
| 1.32 | 1.381 | 37.27 | 62.73 | −0.113 | 1.5982 | 1.5727 | 1.5912 |
| 1.48 | 1.383 | 38.68 | 61.32 | −0.101 | 1.5991 | 1.5725 | 1.5911 |
| 1.64 | 1.379 | 35.62 | 64.38 | −0.094 | 1.5971 | 1.5723 | 1.5882 |
| 1.80 | 1.379 | 35.79 | 64.21 | −0.085 | 1.5972 | 1.5720 | 1.5873 |
| 1.96 | 1.378 | 34.96 | 65.04 | −0.078 | 1.5967 | 1.5718 | 1.5859 |

where $\Phi^{\parallel} = \dfrac{n_{\parallel}^2 - 1}{n_{\parallel}^2 + 2}$ and analogous equation can be derived for $\Phi^{\perp}$, and $(\Delta\alpha \backslash 3\alpha_0)$ is found to be 0.104 for PET, which agrees with previous published results.[28] It can be seen that the value of $[P_2(\theta)]_{opt}$ for the annealed drawn samples are shown as a function of $[DR^2 - DR^{-1}]$. The results are consistent with the deformation of a network with $N_{(2)}$ random links per chain where

$$[P_2(\theta)] = \frac{DR^2 - DR^{-1}}{5N_{(2)}} \qquad (19)$$

where $DR$ is the extension or draw ratio.

**Table III(a) The Polarizability of a Monomer Unit $\alpha^{\parallel}$, $\alpha^{\perp}$, and $\bar{\alpha}$, the Specific Refractivity of the Isotropic Dielectric $\varepsilon^{\parallel}$, $\varepsilon^{\perp}$, and $\bar{\varepsilon}$, at A Constant Annealing Temperature (120 ± 1°C) Quenched in Air**

| Draw Ratio | $\alpha^{\parallel} \times 10^{-33}$ | $\alpha^{\perp} \times 10^{-33}$ | $\bar{\alpha} \times 10^{-33}$ | $\varepsilon^{\parallel} \times 10^{-1}$ | $\varepsilon^{\perp} \times 10^{-1}$ | $\bar{\varepsilon} \times 10^{-1}$ |
|---|---|---|---|---|---|---|
| 1.00 | 2.273 | 1.998 | 2.136 | 2.685 | 2.360 | 2.522 |
| 1.16 | 2.286 | 1.991 | 2.139 | 2.700 | 2.352 | 2.526 |
| 1.32 | 2.319 | 1.974 | 2.146 | 2.738 | 2.331 | 2.535 |
| 1.48 | 2.341 | 1.961 | 2.151 | 2.764 | 2.316 | 2.540 |
| 1.64 | 2.354 | 1.954 | 2.154 | 2.780 | 2.307 | 2.544 |
| 1.8 | 2.364 | 1.949 | 2.156 | 2.791 | 2.301 | 2.546 |
| 1.96 | 2.375 | 1.942 | 2.159 | 2.805 | 2.294 | 2.549 |
| 2.12 | 2.392 | 1.933 | 2.162 | 2.824 | 2.282 | 2.553 |
| 2.28 | 2.404 | 1.926 | 2.165 | 2.839 | 2.274 | 2.556 |

**Table III(b) The Polarizability of a Monomer Unit $\alpha^{\parallel}$, $\alpha^{\perp}$, and $\bar{\alpha}$, the Specific Refractivity of the Isotropic Dielectric $\varepsilon^{\parallel}$, $\varepsilon^{\perp}$, and $\bar{\varepsilon}$, at A Constant Annealing Temperature (140 ± 1°C) Quenched in Air**

| Draw Ratio | $\alpha^{\parallel} \times 10^{-33}$ | $\alpha^{\perp} \times 10^{-33}$ | $\bar{\alpha} \times 10^{-33}$ | $\varepsilon^{\parallel} \times 10^{-1}$ | $\varepsilon^{\perp} \times 10^{-1}$ | $\bar{\varepsilon} \times 10^{-1}$ |
|---|---|---|---|---|---|---|
| 1.00 | 2.287 | 1.991 | 2.139 | 2.701 | 2.351 | 2.526 |
| 1.16 | 2.304 | 1.981 | 2.142 | 2.721 | 2.339 | 2.530 |
| 1.32 | 2.318 | 1.974 | 2.146 | 2.737 | 2.331 | 2.534 |
| 1.48 | 2.320 | 1.972 | 2.147 | 2.741 | 2.329 | 2.535 |
| 1.64 | 2.338 | 1.963 | 2.150 | 2.761 | 2.318 | 2.540 |
| 1.8 | 2.351 | 1.955 | 2.153 | 2.777 | 2.309 | 2.543 |
| 1.96 | 2.356 | 1.953 | 2.155 | 2.783 | 2.306 | 2.544 |
| 2.12 | 2.378 | 1.952 | 2.155 | 2.784 | 2.305 | 2.545 |
| 2.28 | 2.363 | 1.949 | 2.156 | 2.790 | 2.302 | 2.546 |
| 2.44 | 2.370 | 1.945 | 2.157 | 2.798 | 2.297 | 2.548 |

**Table III(c) The Polarizability of a Monomer Unit $\alpha^{\parallel}$, $\alpha^{\perp}$, and $\bar{\alpha}$, the Specific Refractivity of the Isotropic Dielectric $\varepsilon^{\parallel}$, $\varepsilon^{\perp}$, and $\bar{\varepsilon}$, at A Constant Annealing Temperature (160 ± 1°C) Quenched in Air**

| Draw Ratio | $\alpha^{\parallel} \times 10^{-33}$ | $\alpha^{\perp} \times 10^{-33}$ | $\bar{\alpha} \times 10^{-33}$ | $\varepsilon^{\parallel} \times 10^{-1}$ | $\varepsilon^{\perp} \times 10^{-1}$ | $\bar{\varepsilon} \times 10^{-1}$ |
|---|---|---|---|---|---|---|
| 1.00 | 2.306 | 1.981 | 2.143 | 2.723 | 2.339 | 2.531 |
| 1.16 | 2.332 | 1.966 | 2.150 | 2.754 | 2.322 | 2.538 |
| 1.32 | 2.345 | 1.959 | 2.152 | 2.770 | 2.313 | 2.541 |
| 1.48 | 2.364 | 1.948 | 2.156 | 2.792 | 2.301 | 2.546 |
| 1.64 | 2.380 | 1.940 | 2.160 | 2.811 | 2.290 | 2.551 |
| 1.8 | 2.396 | 1.931 | 2.163 | 2.829 | 2.280 | 2.555 |
| 1.96 | 2.409 | 1.922 | 2.166 | 2.845 | 2.271 | 2.558 |

Also, the optical orientation angle can be found by using the following equation:

$$F_{\theta} = 1 - \tfrac{3}{2} \operatorname{Sin}^2\theta \qquad (20)$$

where $\theta$ is the angle between the axis of polymer unit and the fiber axis.

Roe and Krigbaum[29–30] have derived an expression for the distribution of segments at an angle $\theta$ with respect to the draw ratio.

$$\omega(\operatorname{Cos}\theta) = \frac{1}{2} + \frac{1}{4N_{(2)}} (3 \operatorname{Cos}^2\theta - 1) \times \left( DR^2 - \frac{1}{DR} \right) \qquad (21)$$

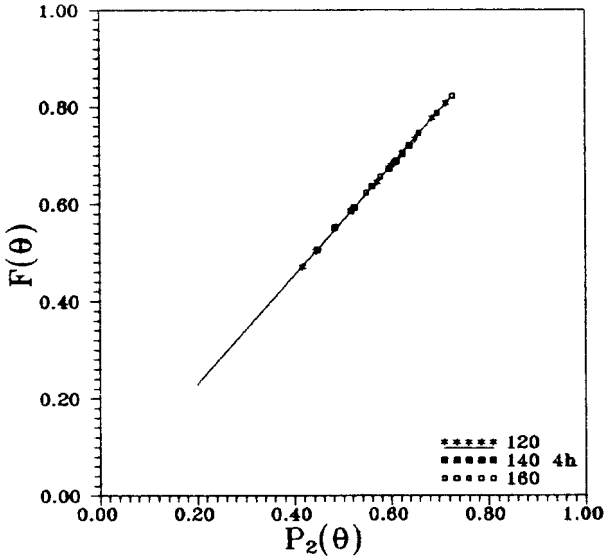


**Figure 2** The relationship between corrected values of optical orientation function $f_\theta$ and the Hermans function $f_\Delta$ of fiber with different draw ratios at 120, 140, and 160°C.

From eq. (21), we found that the distribution of segments change from 0.58 to 0.76.

Before orientation, the segments will be randomly oriented at an angle $\theta$ with respect to the draw direction. After a draw ratio $DR$, the segments will be constrained at an angle $\beta$ given by

$$\tan \beta = DR^{-3/2} \tan \theta \qquad (22)$$

## EXPERIMENTAL RESULTS AND DISCUSSION

Annealing of samples is described in the literature.[15,16]

### Double-Beam Interferometry

A Pluta polarizing interference microscope connected to a device dynamically studies the draw ratio. The values of the birefringence $\Delta n$ and mean refractive indices along $n_a^{\parallel}$ and across $n_a^{\perp}$ of the fiber axis are give in Tables I(a)–(c)

First, we calculated the isotropic refractive index from the following relationship:[31]

$$\frac{n_{\mathrm{iso}(2)}^2 - 1}{n_{\mathrm{iso}(2)}^2 + 2} = \frac{\rho_i}{3\rho}\left[\frac{n_{\parallel}^2 - 1}{n_{\parallel}^2 + 2} + 2\,\frac{n_{\perp}^2 - 1}{n_{\perp}^2 + 2}\right] \qquad (23)$$

where $\rho$ and $\rho_i$ are the density of isotropic unannealed and annealed samples (or drawn or undrawn samples), and $n_a^{\parallel}$, $n_a^{\perp}$ are the refractive indices along and perpendicular to the fiber axis.

### Density Measurement

The density of the unannealed sample was estimated by acoustic method, which have been discussed in details elsewhere.[19,32] The densities of the drawn samples were estimated by using the formula of de Vries and coworkers[33] by the following relation:

$$\rho = 4.047\,\frac{(\bar{n}^2 - 1)}{(\bar{n}^2 + 2)} \qquad (24)$$

where $\bar{n}$ calculated from eq. (10). We have used eq. (24) in our present work for evaluation crystallinity of cold drawn PET fibers because it was the available technique at the present time.

### Degree of Crystallinity

The degree of crystallinity $\chi$ was determined by the following relation:[22]

$$\chi = \frac{\rho - \rho_a}{\rho_c - \rho_a} \qquad (25)$$

with $\rho_c = 1.457 \times 10^3$ kg/m$^3$, and $\rho_a = 1.336 \times 10^3$ kg/m$^3$.

## RESULTS

Plates 1(a)–(c) and 2(a)–(c) show a microinterferograms of totally duplicated images of PET fiber using the Pluta microscope in parallel and perpendicular directions, respectively, with different draw ratios at a constant annealing time of 4 h and different annealing temperatures of 120, 140, and 160 ± 1°C. The refractive index of the immersion liquid was 1.658 and 1.569 at 18 ± 1°C in parallel and perpendicular directions, respectively. Using these interferograms, the mean refractive index of the parallel and perpendicular directions at different draw ratios were calculated. The refractive index of the immersion liquid was selected to allow the fringe shift to be small. Plates 1 and 2 also show that the fringe shifts change as the draw ratio increases and the diameter decreases.

Figures 1(a)–(c) show the relation between the birefringence $\Delta n$ and the refractive index dif-

**Table IV(a) The Orientation Angle $\theta$ and $\theta'$ and Optical Orientation Functions $F_\Delta$, $F_\theta$, at A Constant Annealing Temperature (120 ± 1°C)**

| Draw Ratio | $\theta$ | $\theta'$ | $F_\Delta$ | $F_\theta$ | $F_\theta - F_\Delta/F_\theta$ | $F_\theta/F_\Delta$ |
|---|---|---|---|---|---|---|
| 1.00 | 36.42 | 38.58 | 0.4167 | 0.4712 | 0.1157 | 1.13 |
| 1.16 | 35.11 | 37.50 | 0.4442 | 0.5037 | 0.1183 | 1.13 |
| 1.32 | 31.61 | 34.55 | 0.5175 | 0.5880 | 0.1200 | 1.13 |
| 1.48 | 29.11 | 32.32 | 0.5713 | 0.6451 | 0.1145 | 1.13 |
| 1.64 | 27.52 | 31.06 | 0.6008 | 0.6797 | 0.1161 | 1.13 |
| 1.80 | 26.35 | 30.02 | 0.6246 | 0.7044 | 0.1133 | 1.13 |
| 1.96 | 24.92 | 28.85 | 0.6508 | 0.7337 | 0.1129 | 1.13 |
| 2.12 | 22.69 | 27.21 | 0.6863 | 0.7768 | 0.1166 | 1.13 |
| 2.28 | 20.96 | 25.86 | 0.7146 | 0.8080 | 0.1156 | 1.13 |

**Table IV(b) The Orientation Angle $\theta$ and $\theta'$ and Optical Orientation Functions $F_\Delta$, $F_\theta$, at A Constant Annealing Temperature (140 ± 1°C)**

| Draw Ratio | $\theta$ | $\theta'$ | $F_\Delta$ | $F_\theta$ | $F_\theta - F_\Delta/F_\theta$ | $F_\theta/F_\Delta$ |
|---|---|---|---|---|---|---|
| 1.00 | 35.00 | 37.37 | 0.4475 | 0.5066 | 0.1166 | 1.13 |
| 1.16 | 33.15 | 35.94 | 0.4833 | 0.5515 | 0.1237 | 1.13 |
| 1.32 | 31.72 | 34.58 | 0.5167 | 0.5854 | 0.1175 | 1.13 |
| 1.48 | 31.38 | 34.26 | 0.5246 | 0.5934 | 0.1160 | 1.13 |
| 1.64 | 29.46 | 32.76 | 0.5608 | 0.6371 | 0.1197 | 1.13 |
| 1.80 | 27.84 | 31.25 | 0.5963 | 0.6728 | 0.1138 | 1.13 |
| 1.96 | 27.24 | 30.71 | 0.6088 | 0.6858 | 0.1123 | 1.13 |
| 2.12 | 27.04 | 30.55 | 0.6125 | 0.6900 | 0.1119 | 1.13 |
| 2.28 | 26.45 | 30.02 | 0.6246 | 0.7025 | 0.1109 | 1.13 |
| 2.44 | 25.60 | 29.33 | 0.6400 | 0.7200 | 0.1117 | 1.13 |

**Table IV(c) The Orientation Angle $\theta$ and $\theta'$ and Optical Orientation Functions $F_\Delta$, $F_\theta$, at A Constant Annealing Temperature (160 ± 1°C)**

| Draw Ratio | $\theta$ | $\theta'$ | $F_\Delta$ | $F_\theta$ | $F_\theta - F_\Delta/F_\theta$ | $F_\theta/F_\Delta$ |
|---|---|---|---|---|---|---|
| 1.00 | 33.07 | 35.87 | 0.4850 | 0.5534 | 0.1237 | 1.13 |
| 1.16 | 30.09 | 33.28 | 0.5483 | 0.6230 | 0.1199 | 1.13 |
| 1.32 | 28.59 | 32.02 | 0.5783 | 0.6566 | 0.1193 | 1.13 |
| 1.48 | 26.33 | 30.05 | 0.6238 | 0.7050 | 0.1153 | 1.13 |
| 1.64 | 24.29 | 28.47 | 0.6592 | 0.7462 | 0.1166 | 1.13 |
| 1.80 | 22.15 | 26.72 | 0.6967 | 0.7867 | 0.1145 | 1.13 |
| 1.96 | 20.14 | 25.16 | 0.7288 | 0.8222 | 0.1137 | 1.13 |

ferences ($n^\parallel - n_v$, $n^\perp - n_v$, $n^\parallel - n_{iso}$, and $n^\perp - n_{iso}$). In Figure 1, $n_v$ and $\Delta n_{max}$ are used to predict the values of refractive indices, $n_1$ and $n_2$, for fully oriented fibers. These values are found to be 1.80 and 1.56, respectively, at 28°C, which are in agreement with the published values.[24]

Tables I(a)–(c) give some experimental results for annealed PET fibers, refractive indices, and the calculated values of the number of molecular per unit volume $N$, and random links per chain ($N_{(2)}$).

The apparent volume fraction of crystallinity ($\chi$) was calculated from eq. (25) using the calculated density values. The results are given in Tables II(a)–(c). Also in Tables II(a)–(c) are the calculated values of $1 - \chi$, virtual refractive index ($n_v$), the form birefringence ($\Delta n_f$), and isotropic refractive index, which were calculated using eqs. (10) and (23), respectively.

In Tables III(a)–(c), the calculated values of $\alpha^\parallel$, $\alpha^\perp$, and $\alpha$, and the specific refractivity of the isotropic dielectric of parallel, perpendicular, and

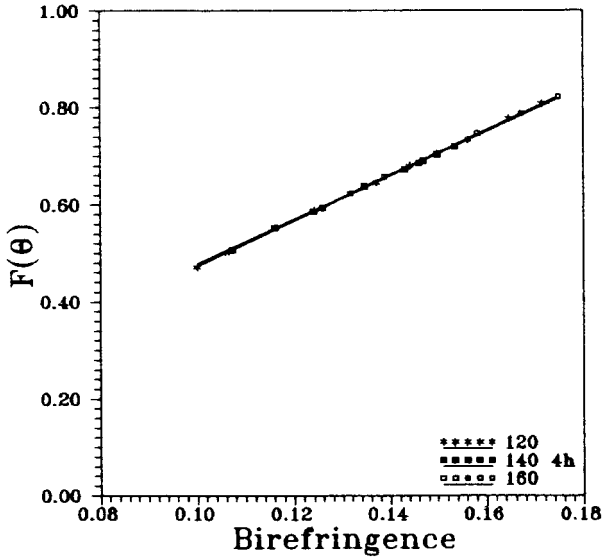


**Figure 3** The relationship between $\langle P_2(\theta)\rangle$ and birefringence $\Delta n_a$ of fiber with different draw ratios at 120, 140, and 160°C.

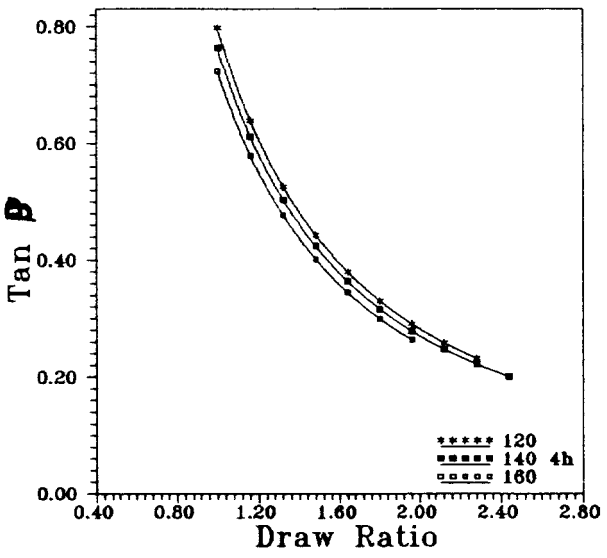


**Figure 5** The relation between tan $\beta$ and different draw ratios at 120, 140, and 160°C.

mean value ($\epsilon^{\parallel}$, $\epsilon^{\perp}$, and $\bar{\epsilon}$) at different draw ratios are given, for annealed PET fibers.

Figure 2 shows the relation between corrected values of optical orientation function $f_\theta$ and the Hermans function $f_\Delta$ for different draw ratios for annealed fibers at 3 annealing temperatures, from which $f_\theta/f_\Delta$ is found to be 1.13 for 120, 140, and 160°C. The calculated values of the orientation angle $\theta$ from $f_\theta$ and $\theta'$ from $f_\Delta$ and at different draw ratios are given in Table IV(a)–(c).

Figure 3 shows the relation between the birefringence $\Delta n$ and the optical orientation function $f_\theta$ for various draw ratios of annealed fibers.

Figure 4 shows the relation between $\langle P_2(\theta)\rangle$ and $[DR^2 - DR^{-1}]$, which is a straight line; from it, we calculated the values of random links per chain ($N_{(2)}$).

Figure 5 shows the relation between tan $\beta$ and draw ratios at different annealing temperatures and a constant annealing time of 4 h. Tan $\beta$ decreases with increasing draw ratio.

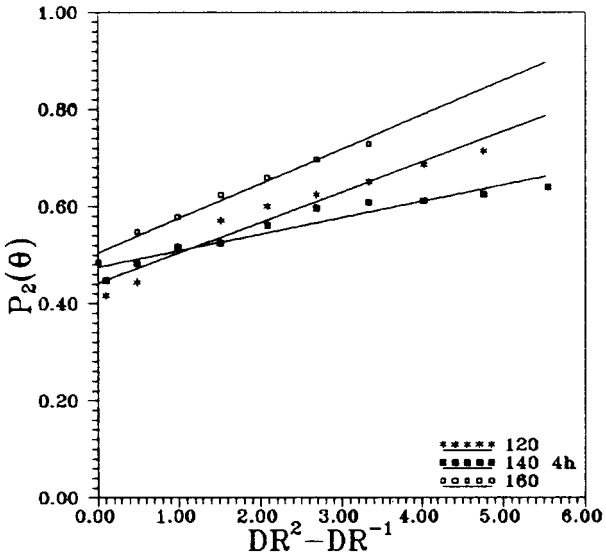


**Figure 4** The relationship between $\langle P_2(\theta)\rangle$ and $[DR^2 - DR^{-1}]$ of fiber at 120, 140, and 160°C.

## DISCUSSION

Characterization of synthetic polymer fibers are important for the main end use. Birefringence, orientation, density, crystallinity, and elasticity are some of the needed properties that affect the textile quality. Most studies that involve variations of physical properties considered polymers as an anisotropic polycrystalline medium, that is, consisting of crystalline regions suspended in an amorphous medium, which is partially oriented.[32]

The formation of a crystal lattice in a polymer restricts the mobility of the segments; with an increase in the degree of crystallinity, a polymer therefore becomes more rigid. On the other hand, an increase in the amorphous part increases the ability to deform.

So thermal and mechanical treatments are used to vary the degree of orientation, crystallinity, and other physical properties in polymeric materials. Also, to explain the different variations obtained due to thermomechanical effects, there are several structural processes interfered with that should be in consideration, which are discussed elsewhere.[34–36]

## CONCLUSIONS

From the previous results and representations, the following conclusions may be drawn.

1. Two-beam interferometry and acoustic techniques can provide accurate measures and evaluation of overall molecular orientation in PET.
2. The combination of measurements of birefringence and optical parameters with crystallinity index can throw light on the evaluation of the form birefringence and the deformation mechanism occurring due to cold drawing effect.
3. It is interesting to note that the parameter $N$ changes significantly with increasing draw ratio, perhaps representing the slippage in the network required by a transition from affine to pseudoaffine deformation.
4. It is clear that $\alpha = 0.9$ is constant whatever the physical process affecting the fiber.
5. It is clear that there are changes in the calculated values of the isotropic refractive indices due to application of different formulae. By comparison, it is found $n_v \cong n_{\mathrm{iso}_{(1)}}$, but the obtained values by eq. (23) are different due to its derivation that include density parameter, which is related to the degree of crystallinity of the principal structural parameter. We do not claim that its application is preferable, but every equation has its own merit.
6. The form birefringence cannot be neglected and must be considered to throw light on the phase boundary between the amorphous and crystalline regions.

The authors thank Prof. A. A. Hamza, the President of Mansoura University, for useful discussions.

## REFERENCES

1. N. Barakat, *Text. Res. J.,* **41,** 391 (1971).
2. N. Barakat and A. A. Hamza, *Interferometry of Fibrous Materials,* Hilger, Bristol, 1990.
3. J. R. Samules, *Structural Polymer Properties,* Vol. 20, Wiley, New York, 1974, pp. 50–60.
4. I. M. Fouda, M. M. El-Tonsy, and H. M. Hosny, *Polym. Degrad. Stab.,* **46,** 287 (1994).
5. I. M. Fouda and M. M. El-Tonsy, *J. Mater. Sci.,* **25,** 121 (1990).
6. A. A. Hamza, I. M. Fouda, M. A. Kabeel, and H. M. Shabana, *Polym. Test.,* **15,** 35 (1996).
7. I. M. Fouda and E. A. Seisa, *J. Polym., Polym. Comp.,* **4,** 247 (1996).
8. I. M. Fouda, M. M. EL-Nicklawy, E. M. Naser, and R. M. EL-Agamy, *J. Appl. Polym. Sci.,* **60,** 1247 (1996).
9. M. F. Vallat, D. J. Plazek, and B. Bhushan, *J. Polym. Sci., Part B: Polym. Phys.,* **26,** 555 (1988).
10. A. A. Hamza, T. Z. N. Sokkar, and M. A. Kabeel, *J. Phys. D: Appl. Phys.,* **18,** 2321 (1985).
11. A. A. Hamza, K. A. EL-Farahaty, and S. A. Helaly, *Opt. Applic.,* **18,** 133 (1988).
12. A. H. Oraby and M. A. Mabrouk, *Polym. Test.,* **14,** 439 (1995).
13. I. M. Fouda and E. A. Seisa, *J. Polym., Polym. Comp.,* **4,** 489 (1996).
14. I. M. Fouda, M. M. EL-Nicklawy, A. F. Hassan, and A. M. EL-Kelany, *Polym. Int.,* **38,** 233 (1995).
15. A. A. Hamza, I. M. Fouda, M. A. Kabeel, E. A. Seisa, and F. M. El-Sharkawy, *Polym. Test.,* to appear.
16. A. A. Hamza, I. M. Fouda, M. A. Kabeel, E. A. Seisa, and F. M. El-Sharkawy, *J. Appl. Polym. Sci.,* to appear.
17. M. Pluta, *J. Opt. Acta,* **18,** 661 (1971).
18. M. Pluta, *J. Microsc.,* **96,** 309 (1972).
19. A. A. Hamza, I. M. Fouda, M. M. EL-Tonsy, and F. M. El-Sharkawy, *J. Appl. Polym. Sci.,* **56,** 1355 (1995).
20. V. A. Sarkisyan, M. G. Asratyan, A. A. Mkhitoryan, K. KH. Katrdzhyan, and A. K. Dadivanyan, *Vysokomal. Sayed,* **A27,** 1331 (1985).
21. F. Happy, *Applied Fiber Science,* Vol. 1, Academic Press, London, 1983, p. 130.
22. G. L. Bourvelles and J. Beautemps, *J. Appl. Polym. Sci.,* **39,** 329 (1990).
23. A. D. Jenkins, *Polymer Science: A Materials Science Handbook,* Vol. 1, North Holland, Amsterdam, 1972, Chap. 7, p. 496.
24. H. de Vries, *Z. Colloid, Polym. Sci.,* **257,** 226 (1979).
25. P. H. Hermans, *Contributions to the Physics of Cellulose Fibers,* North Holland, Amsterdam, 1946.
26. I. M. Ward, *J. Polym. Sci., Polym. Symp.,* **53,** 9 (1977).
27. A. Cunningham, G. R. Davies, and I. M. Ward, *Polymer,* **15,** 743 (1974).
28. I. M. Perena, A. A. Duckett, and I. M. Ward, *J. Appl. Polym. Sci.,* **25,** 1381 (1980).
29. R. J. Roe and W. R. Krigbaum, *J. Appl. Phys.,* **35,** 2215 (1964).

30. D. J. Blundell, A. Mahendrasingam, D. McKeron, A. Turner, R. Rule, R. J. Oldman, and W. Fuller, *Polymer,* **35,** 3875 (1994).
31. A. Cunningham, I. M. Ward, H. A. Willis, and V. Zichy, *Polymer,* **15,** 749 (1974).
32. I. M. Fouda, M. M. El-Tonsy, and A. M. Shaban, *J. Mater. Sci.,* **26,** 5085 (1990).
33. A. J. de Vries, C. Bonnebat, and Beatutemps, *J. Polym. Sci. Polym. Symp.,* **58,** 109 (1977).
34. P. Polukhin, S. Gorelik, and V. Vortontsov, *Physical Principals of Plastic Deformation,* Mir, Moscow, 1983, p. 275.
35. E. A. and S. R. Porter, *The Strength and Stiffness of Polymers,* Marcel Dekker, New York, 1983, p. 121.
36. D. C. Bassett, *Principles of Polymer Morphology,* Cambridge University Press, Cambridge, 1981, p. 124.